



# Investigation of Annealing Effect on Characteristics of Nickel–Boron Alloy Thin Films

Dr.T.Baskar<sup>1</sup>, Dr.A.Shaji George<sup>2</sup>

<sup>1</sup>Professor, Department of Physics, Shree Sathyam College of Engineering and Technology, Sankari Taluk, Salem District, Tamil Nadu, India.

<sup>2</sup>Almarai Company, TSM, Business System Department, Kingdom of Saudi Arabia.

**Abstract** – Ni-B alloy thin films were fabricated through room temperature electroplating, followed by annealing at 200°C. The electroplated Ni-B thin films exhibited a preferred orientation with a face-centered cubic (FCC) phase. Comprehensive analyses were conducted to assess the morphological, structural, and mechanical characteristics of the Ni-B films. These films displayed a bright and uniform coating on the surface, with nano-scale deposits and an average crystalline size of approximately 95 nm. Following annealing, the microhardness of the Ni-B films reached 221 Vickers hardness number (VHN).

**Keywords:** Electroplating, electrolytic bath, crystalline size, VSM, Ni-B, X-ray diffraction, VHN, SEM.

## 1. INTRODUCTION

Ni-B electrodeposits serve as a viable alternative to conventional Ni electrodeposits, benefitting from the microstructure-refining role of cobalt, leading to enhanced characteristics and a decreased reliance on organic grain refiners [1-5]. The widespread use of Ni-B, B-Co, and B-Fe alloys is attributed to their favorable combination of low coercivity and high saturation magnetization. Given that the magnetic properties of Ni-B alloys are significantly influenced by their crystal structure, a comprehensive examination of this engineering material is essential for its various applications [6-10]. This study focuses on investigating the impact of annealing on Ni-B films.

## 2. EXPERIMENTAL PART

Ni-B alloy films were electrodeposited using an electrolyte solution comprising Borax (15 g/l), Nickel sulfate (30 g/l), Ammonium sulfate (40 g/l), Boric acid (10 g/l), and Saccharin (10 g/l), with the process conducted at a temperature of 30°C. The deposition, utilizing copper and stainless steel substrates (1.5 cm x 7.5 cm) as cathode and anode, respectively, lasted for 15 minutes [10-14]. To adjust the pH to 6.0, ammonia solution was added, and the electroplating proceeded with a current density of 3 mA/cm<sup>2</sup>. After 15 minutes, the copper cathode was carefully withdrawn from the bath and allowed to dry for a few minutes [14-17]. Subsequently, the electroplated Ni-B thin films underwent annealing at 200°C.

## 3. RESULTS AND DISCUSSION

### 3.1 Elemental Composition of Nib Thin Films

The elemental composition of Ni-B films was analyzed using an EDAX analyzer, and the resulting data is presented in Table 1. The analysis revealed that, following the annealing process, there was an increase in boron content accompanied by a decrease in nickel content.

**Table -1:** EDAX analysis of thin films

S. No	Condition	Co Wt%	Ni Wt%
1.	Ni-B (30°C)	34.34	65.66
2	Ni-B (Annealed 200°C)	36.72	63.28

### 3.2. Morphological Observation

The surface appearance of Ni-B thin films at 30°C and the annealed thin film was examined using Scanning Electron Microscope (SEM) images, as depicted in Fig 1. The thin films exhibit a bright and uniform coating on the surface, displaying an absence of cracks in their appearance.

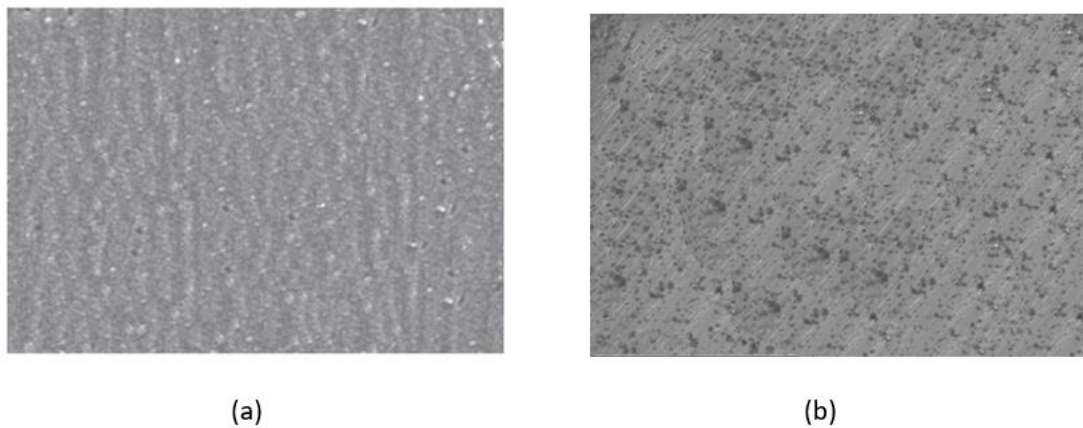


**Fig -1:** SEM images of thin films (a) Ni-B (30°C) (b) Ni-B (Annealed 200°C)

### 3.3. Structural Characters

The structural characteristics, derived from XRD data, of the deposited materials prepared at a temperature of 30°C and the annealed thin film are presented in Figure 2. The XRD pattern of Ni-B indicates the formation of crystals in the deposits. The results reveal a face-centered cubic phase with three distinct diffraction peaks in the XRD pattern of Ni-B films, confirming the presence of nano-crystallite deposits. The crystallite sizes of Ni-B deposits are tabulated in table 2. Annealing process decreases the crystal size.

**Table -2:** Ni-B alloy films -Structural properties

S.No	Condition	2θ (deg)	d (Å)	Particle Size(D) (nm)
1	Ni-B (30°C)	42.94	1.7341	90.35
2	Ni-B (Annealed 200°C)	41.78	1.6671	99.81

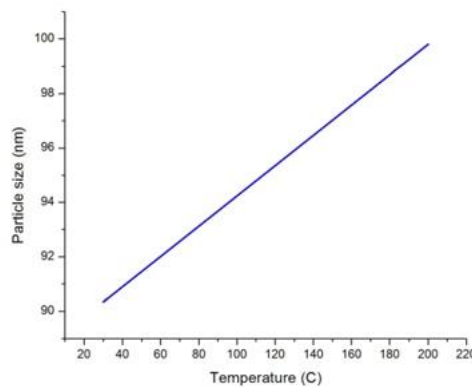


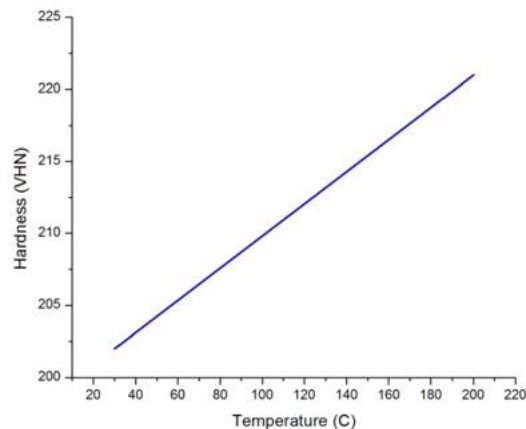
**Fig -2:** Particle size changes with condition

### 3.4. Mechanical Properties

Microhardness measurements of the deposits were conducted using a Vickers hardness tester, and the hardness values for thin films at room temperature (30°C) and the annealed thin film are provided in Table 3. The results indicate that the annealing process leads to an increase in hardness. This can be attributed to the initiation of crystal deposit formation during the electro-deposition process.

**Table -3:** Ni-B alloy films -Hardness

S.No	Condition	Hardness VHN)
1	Ni-B (30°C)	202
2	Ni-B (Annealed 200°C)	221

**Fig -3:** Hardness changes with condition

#### 4. CONCLUSION

Ni-B alloy thin films were fabricated through the electro-deposition method, and various characteristics of the resulting films were examined. Analysis of the EDAX data revealed an increase in boron content and a decrease in nickel after the annealing process. The XRD results indicated the presence of a face-centered cubic phase in Ni-B films, as evidenced by three distinct diffraction peaks. Additionally, the thin films prepared with the annealing process exhibited a bright and uniform coating on the surface, appearing free of cracks. Furthermore, microhardness measurements showed an increase in hardness values for the thin films after the annealing process.

#### REFERENCES

- [1] Myung, N. (2001). A Study on the Electrodeposition of NiFe Alloy Thin Films Using Chronocoulometry and Electrochemical Quartz Crystal Microgravimetry, *Bull. Bull. Korean Chem. Soc*, 22, 994–998.
- [2] Sulztanu, N., & Fbrinza, J. (2004). Electrodeposited Ni-Fe-S films with high resistivity for Magnetic recording devices. *J. Optoelectron Adv Mat*, 6, 641–645.
- [3] Kannan, R., Ganesan, S., & Selvakumari, T. M. (2012). Synthesis and characterization of nano crystalline NiFeWS thin films in diammonium citrate bath. *Digest Journal of Nanomaterials and Biostructures*, 7, 1039–1050.
- [4] Yao, C.-Z., Zhang, P., Liu, M., Li, G.-R., Ye, J.-Q., Liu, P., & Tong, Y.-X. (2008). Electrochemical preparation and magnetic study of Bi-Fe-Co-Ni-Mn high entropy alloy. *Electrochemical Acta*, 53(28), 8359–8365. doi:10.1016/j.electacta.2008.06.036
- [5] Gupta, Nutan, Verma, A., Kashyap, S. C., & Dube, D. C. (2005). Dielectric behavior of spin-deposited nanocrystalline nickel-zinc ferrite thin films processed by citrate-route. *Solid State Communications*, 134(10), 689–694. doi:10.1016/j.ssc.2005.02.037
- [6] Chen, Y., Wang, Q. P., Cai, C., Yuan, Y. N., Cao, F. H., Zhang, Z., & Zhang, J. Q. (2012). Electrodeposition and characterization of nanocrystalline CoNiFe films. *Thin Solid Films*, 520(9), 3553–3557. doi:10.1016/j.tsf.2012.01.007
- [7] Emerson, R. N., Kennady, C. J., & Ganesan, S. (2007). Effect of Organic additives on the Magnetic properties of Electrodeposition of CoNiP Hard Magnetic Films. *Thin Solid Films*, 515, 3391–3396.
- [8] Chih-Huang, L., Matsuyama, H., White, R. L., & Anthony, T. C. (1995). Anisotropic exchange for NiFe films grown on epitaxial NiO. *IEEE Transactions on Magnetics*, 31(6), 2609–2611.
- [9] Esther, P., & Joseph Kennady, C. (2010). Effect of sodium tungstate on the properties of Electrodeposited nanocrystalline NiFeCr films. *Journal of Non Oxide Glasses*, 1, 35–44.



- [10] Motomura, Y., Tatsumi, T., Urai, H., & Aoyama, M. (1990b). Soft magnetic properties and heat stability for Fe/NiFe super lattices. *IEEE Transactions on Magnetics*, 26, 2327–2331.
- [11] Motomura, Y., Tatsumi, T., Urai, H., & Aoyama, M. (1990a). Soft magnetic properties and heat stability for Fe/ NiFe super lattices. *IEEE Transactions on Magnetics*, 26, 2327–2331.
- [12] Hamid, Z. A. (2003). Electrodeposition of Cobalt- Tungsten Alloys from Acidic Bath Containing Cationic Surfactants. *Materials Letters*, 57.
- [13] Gupta, N., Verma, A., & Kashyap, S. C. (2005). Dielectric behavior of spin-deposited nano crystalline nickel-zinc ferrite thin films processed by citrate-route. *Solid State Commun*, 10, 689–694.